ChemComm

COMMUNICATION

View Article Online
View Journal | View Issue

Cite this: *Chem. Commun.*, 2019, 55, 834

Received 31st October 2018,
Accepted 12th December 2018

DOI: 10.1039/c8cc08685k

rsc.li/chemcomm

Minimalist linkers suitable for irreversible inhibitors in simultaneous proteome profiling, live-cell imaging and drug screening†

Cuiping Guo,‡[a] Yu Chang,‡[a] Xin Wang,[a] Chengqian Zhang,[b] Piliang Hao,*[b] Ke Ding[a] and Zhengqiu Li *[a]

Activity-based protein profiling (ABPP) and bioimaging have been powerful approaches for *in situ* drug screening and target identification. However, these approaches are still hindered by the preparation of high-quality probes. To address this challenge, we developed a series of novel minimalist linkers for irreversible inhibitors by incorporation of various bioorthogonal handles into an α,β-unsaturated amide, a common moiety of many irreversible inhibitors. The linker-containing probes have been demonstrated to be suitable for simultaneous protein labelling, live cell imaging and drug screening.

Drug screening and target identification are critical steps in drug discovery, but they rely mainly on traditional *in vitro* enzymatic assays, which often must first be developed.[1] To solve this problem, activity-based protein profiling (ABPP) and bioimaging have been developed recently as powerful and complementary approaches that can be applied for both target identification and drug screening in native environments.[2] A large number of lead compounds and potential druggable targets have been identified singly or collectively through these approaches.[3] However, both approaches are still hindered by the lack of high quality probes capable of recapitulating genuine drug–target engagement. This can be accounted for by different elements such as bioorthogonal handles, fluorophores and/or photo-crosslinkers, which must be embedded in the parent molecules with minimal perturbation of the original binding sites. We recently developed several types of photo-crosslinkers with bioorthogonal handles for reversible inhibitors in affinity-based proteome profiling (AfBP) and bioimaging studies (Fig. 1A).[4] Owing to the improved synthesis of photoprobes, which enable simultaneous protein labeling and cellular imaging, they have been broadly applied in various small molecules for target identification.[5] In this work, we endeavored to create a series of minimalist linkers for irreversible inhibitors (Fig. 1B), with the aim to facilitate the synthesis of activity-based probes and enable simultaneous imaging of endogenous kinase activities, studying target engagement in live cells, and drug screening against druggable targets such as EGFR and BTK.

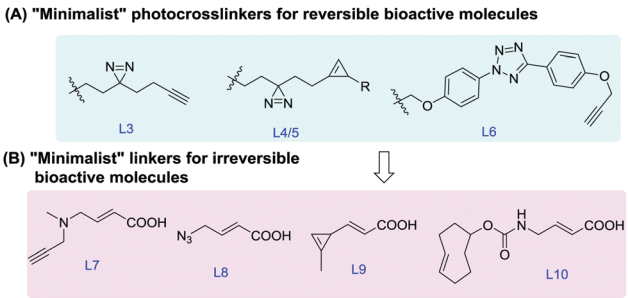

Fig. 1 Structures of minimalist linkers for (A) reversible inhibitors and (B) irreversible inhibitors, respectively.

With this goal in mind, we examined the structures of various irreversible inhibitors and observed that most of them, especially kinase inhibitors, possess an α,β-unsaturated amide. Importantly, this common moiety is tolerable for modification based on previously reported structure–activity relationships (SAR)[6] and the co-crystal structures of molecules with proteins (Fig. S1, ESI†).[7] Thus, we postulated that incorporation of bioorthogonal handles, especially copper-free ones such as azide, cyclopropene, or *trans*-cyclooctene (TCO), into an α,β-unsaturated carboxylic acid could produce minimalist-size linkers (Fig. 1B), which could confer better bioactivities and dual functions on the corresponding probes, thus supporting proteome profiling and live-cell imaging.

To prove this idea, we incorporated linkers into representative irreversible inhibitors, afatinib and ibrutinib, to assess

[a] *School of Pharmacy, Jinan University, Guangzhou City Key Laboratory of Precision Chemical Drug Development, International Cooperative Laboratory of Traditional Chinese Medicine Modernization and Innovative Drug Development, Ministry of Education (MOE) of People's Republic of China, 601 Huangpu Avenue West, Guangzhou, 510632, China. E-mail: pharmlzq@jnu.edu.cn*

[b] *School of Life Science and Technology, ShanghaiTech University, 393 Middle Huaxia Road, Shanghai 201210, China. E-mail: haopl@shanghaitech.edu.cn*

† Electronic supplementary information (ESI) available. See DOI: 10.1039/c8cc08685k

‡ Cuiping Guo and Yu Chang contributed equally to this work.

(A)

Chemical structures	Parent inhibitor and probes		Chemical structures	Parent inhibitor and probes	
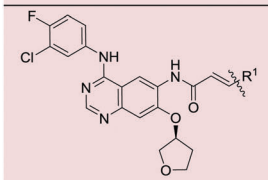	**afatinib** (R^1 =)	**AF-1** (R^1 =)	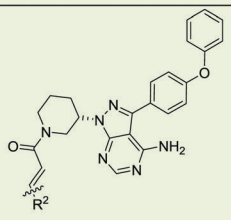	**ibrutinib** (R^2 =) -H	**IB-1** (R^2 =)
		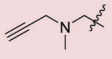			
		AF-2 (R^1 =)		**IB-2** (R^2 =)	**IB-3** (R^2 =)
				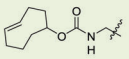	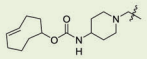

(B)

IC_{50}	afatinib	AF-1	AF-2	IC_{50}	ibrutinib	IB-1	IB-2	IB-3
$EGFR^{WT}$ *(nM)*	0.37±0.06	0.64±0.18	0.63±0.06	*BTK (nM)*	1.68±0.27	75.0±11.1	21.5±4.20	6.33±0.57
$EGFR^{T790M}$ *(nM)*	2.54±0.13	8.18±1.81	5.08±0.42	*Raji cells (μM)*	6.46±3.28	12.08±4.16	9.93±5.41	1.81±0.9
A431cells (μM)	2.29±0.3	7.79±0.1	5.02±0.1	*A431 cells (μM)*	14.96±1.8	37.75±8.66	29.88±0.91	6.06±1.28

Fig. 2 (A) Chemical structures of the activity-based probes (ABPs) and parent inhibitors. (B) IC_{50} values of the probes against recombinant proteins and cancer cells with the parent inhibitors as positive controls.

whether they could display desired functions. The introduction of linkers for each molecule was based on previously reported structure–activity relationships.[6] Consequently, **AF-1–2** and **IB-1–3** were readily produced by coupling of commercially available intermediates with the linkers (Fig. 2A and Schemes S1–S5, ESI†), and were fully characterized prior to biological evaluation.

With these probes, we first evaluated their biological activities in comparison with those of their parental inhibitors using standard *in vitro* kinase inhibition assays and cell-based, CCK-8 antiproliferation assays. As shown in Fig. 2B and Fig. S2 (ESI†), **AF-1–2** and **IB-2–3** showed comparable inhibition to the corresponding parent inhibitors under both settings, suggesting that the introduction of these bioorthogonal handles had little effect on protein binding, under *in vitro* and cellular conditions. In contrast, the probe containing cyclopropene (**IB-1**) appeared to be significantly less potent than the parent ibrutinib, implying that cyclopropene is not a suitable substitute for the α,β-unsaturated amide electrophile. This phenomenon could be accounted for by lacking a nitrogen atom in the cyclopropene moiety, as the nitrogen atom is essential for Michael addition by deprotonating the attacking thiol group.

Next, we determined if the newly developed chemical probes could be used in simultaneous protein labeling and bioimaging. After incubation of **AF-1–2** and **IB-1–3** with the corresponding kinase positive cells (A431, Toledo/Raji) for 2–4 h, respectively, the cells were lysed. The resulting cell lysates were conjugated with the corresponding reporters (TAMRA-alkyne, TAMRA-N_3 or tetrazine-Cy5, Table S2, ESI†), and separated by SDS-PAGE, followed by in-gel fluorescence scanning. As shown in Fig. 3A–C and Fig. S3 (ESI†), the samples treated with **AF-1–2** and **IB-2–3** showed a highly selective probe labeling profile, with strong fluorescence labeled bands predominantly at ~170 kDa and ~70 kDa, respectively, indicating excellent target selectivity. In the presence of a ten-fold excess of the parent molecules as competitors, the major fluorescence bands disappeared (Fig. 3A–C and Fig. S3, ESI†), indicating that they were probe-targeted proteins rather than the results of non-specific labeling. Concentration-dependent labeling experiments proved that the specific labeling band is visible at a probe concentration as low as 1 nM, showing that the probes exhibit excellent sensitivity (Fig. S3, ESI†). Consistent with the inhibition assay results, the **IB-1**-treated samples failed to show the corresponding labeling band (Fig. 3B and C). The major labeling bands were proven to be EGFR and BTK, respectively, by pull-down/western blotting with the corresponding antibodies (Fig. 3D).

To assess whether the probes could behave as imaging probes to track target location, cellular imaging of live A431 and Toledo cells with **AF-1–2** and **IB-2–3**, respectively, was carried out. The cells were first treated with the probes for 2–4 h. Subsequently, the cells treated with **AF-1** were fixed, permeabilized and reacted with TAMRA-N_3 under previously optimized click chemistry conditions.[4] The cells treated with **AF-2** and **IB-2–3** were incubated with dibenzocyclooctyne-TAMRA (DBCO-TAMRA) or tetrazine-Cy5 and then imaged directly. Strong fluorescence signals were observed in the cell membrane or the cytoplasm (Fig. 3E). Control imaging experiments with DMSO under similar conditions showed minimal background fluorescence when compared to the labeled cells. Immunofluorescence experiments revealed that the probes were largely co-localized with the target proteins, EGFR and BTK, respectively (Fig. 3E). These lines of evidence proved that the probes are suitable for simultaneous proteome profiling and live-cell imaging.

Finally, we proceeded to identify potential cellular targets of afatinib by large-scale chemoproteomics experiments with **AF-1–2**. As described above, the probe-labeled proteins were affinity-purified and identified by LC-MS/MS analysis. Control experiments were carried out concurrently with afatinib-treated samples, which were used to distinguish real targets from background labeling. A submicromolar probe concentration (0.1 μM) was used to simulate drug action *in situ*. The identified protein hits were optimised with label free quantification (LFQ), and the proteins that appeared in duplicate runs and whose LFQ intensity ratios from the probe-treated and competitive labeling experiments (**AF-1** *vs.* [**AF-1** + afatinib(5×)], or **AF-2** *vs.* [**AF-2** + afatinib(5×)]) were greater than 1.5 were considered further. Finally, 48 and 32 protein hits were positively identified by **AF-1** and **AF-2**, respectively, and ~38% of these proteins were identical (12 of 32, Fig. 3F, G and Table S3, ESI†). The difference

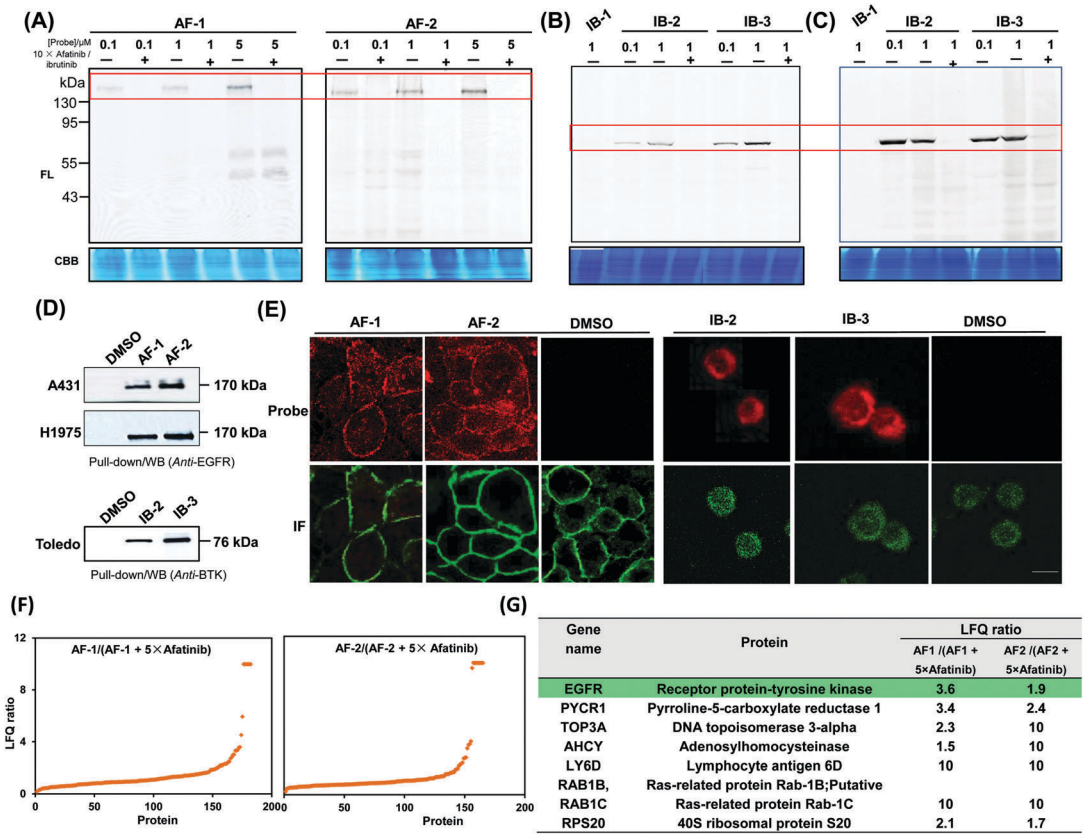

(G)

Gene name	Protein	LFQ ratio	
		AF1 /(AF1 + 5×Afatinib)	AF2 /(AF2 + 5×Afatinib)
EGFR	Receptor protein-tyrosine kinase	3.6	1.9
PYCR1	Pyrroline-5-carboxylate reductase 1	3.4	2.4
TOP3A	DNA topoisomerase 3-alpha	2.3	10
AHCY	Adenosylhomocysteinase	1.5	10
LY6D	Lymphocyte antigen 6D	10	10
RAB1B,	Ras-related protein Rab-1B;Putative		
RAB1C	Ras-related protein Rab-1C	10	10
RPS20	40S ribosomal protein S20	2.1	1.7

Fig. 3 (A–C) Proteome reactivity profiles of live A431 cells treated with **AF-1–2**, Toledo cells treated with **IB-1–3** and Raji cells treated with **IB-1–3**, in the presence or absence of competitors. (D) Pull-down/WB results for target validation of **AF-1–2** and **IB-2–3** in live cells (*in situ*). (E) Live-cell imaging of A431 cells with **AF-1–2** (1 μM probe concentration), and Toledo cells with **IB-2–3** (1 μM). Immunofluorescence (IF) staining using anti-EGFR and anti-BTK antibodies. Scale bar = 10 μm. (F) MS-based identification of proteins enriched by probes **AF-1–2**, ABPP experiments in A431 cells treated with the probes (**AF-1–2**; 0.1 μM, 4 h) in the presence or absence of afatinib; data represent the mean LFQ ratio value for the proteins from duplicate runs. The probe-enriched targets are defined as those with mean LFQ ratio values ≥1.5 (probe/(probe + competitor)). (G) Selected high-confidence proteins enriched with **AF-1–2** (0.1 μM) from live A431 cells simultaneously.

could be accounted for by different linkers and the intrinsic variability of the instruments. Interestingly, the overlapping proteins include the known target (EGFR) and a series of unknown protein targets, such as RAB1B, RAB1CI, TOP3A, PYCR1, AHCY and LY6D, which could be the potential cellular off-targets of afatinib. These protein hits might be the reason for the anticancer and toxic effects of afatinib. These data together proved that the probes **AF-1**/**AF-2** are suitable to be applied in target identification of thiol-reactive inhibitors by chemoproteomics studies.

Observing that **AF-1**/**AF-2** and **IB-2**/**IB-3** specifically label and image the target proteins, EGFR and BTK, *in situ*, we envisioned that competitive labeling and competitive imaging could be developed as general methods for *in situ* drug screening against these druggable targets. To test this idea, **IB-3** was used as a tool probe to test the inhibition of members of a ~210-membered compound library against BTK with Toledo cells. The compound library consists of commercially available natural products and synthetic small molecules. Upon incubation of **IB-3** with or without the screening inhibitors for 4 h, the cells were lysed and conjugated with tetrazine-Cy5, and the labeled proteomes were separated by SDS-PAGE, and the fluorescence intensity of the BTK band exhibited by **IB-3** was measured. As shown in Fig. 4A and Fig. S4 (ESI†), three compounds, **36** (U73122), **42** and **43**, were identified by screening, which decrease the probe labeling of BTK (* marked band), implying that they are potent inhibitors *in situ*. Similar phenomena were also observed in competitive imaging experiments (Fig. 4B). Further validation of the inhibitory properties revealed IC_{50} values of 4.14 μM, 1.87 nM, 0.13 μM for the three compounds against BTK, respectively (Fig. 4C). The cell-based assay also confirmed the potent inhibition of these screening hits against cancer cells (Fig. S2, ESI†). The effects of the positive screening hits on the BTK signaling pathway also confirmed that these compounds can dose-dependently suppress the phosphorylation of BTK-downstream proteins (Fig. 4D). It is noteworthy that U73122 is a potent phospholipase C (PLC) inhibitor,[8] which reduces agonist-induced Ca^{2+} increase in platelets and polymorphonuclear neutrophils (PMNs), and little information is available to date concerning its inhibitory action against BTK. Compounds **42** and **43** are specific inhibitors against $EGFR^{T790M}$, which were previously developed by our group.[9] These results show that BTK is an off-target of these inhibitors. Taken together, these data show that the minimalist-linker containing probes can be used in simultaneous protein labeling, live cell imaging and *in situ* drug screening.

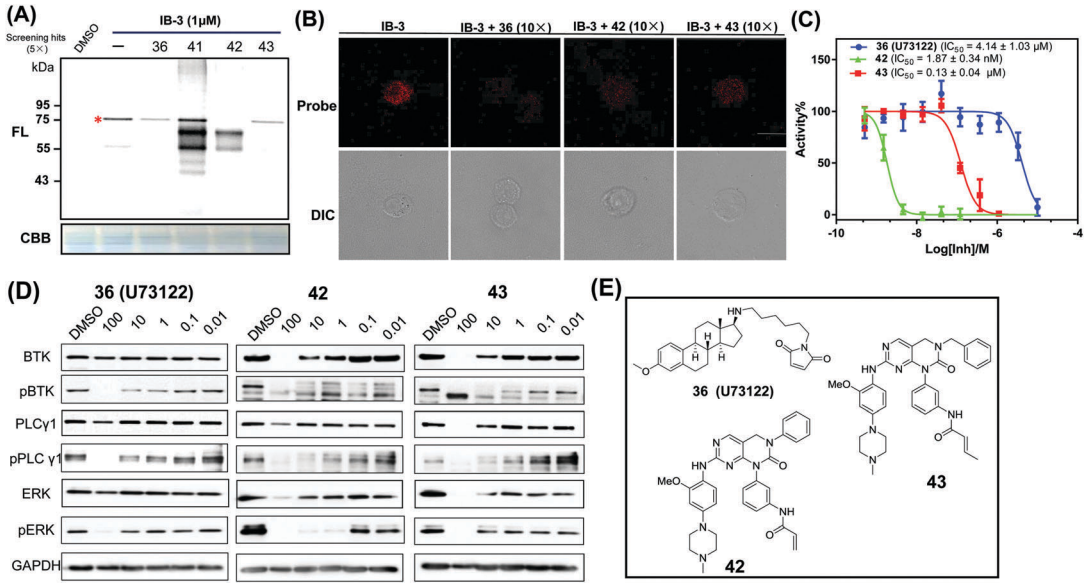

Fig. 4 (A) *In situ* drug screening by competitive labeling with **IB-3** (1 μM), lane 1 is a DMSO control, lane 2 is a positive control, and lanes 3–6 are treated with screening compounds (10 μM final). (B) Competitive imaging of **IB-3** (1 μM) in the presence or absence of screening compounds (10 μM final). (C) IC_{50} values of the positive screening hits against BTK. (D) The effects of the positive screening hits on the phosphorylation of BTK-downstream proteins. (E) Chemical structures of the positive screening hits.

We have developed a series of minimalist linkers for irreversible inhibitors. Upon introduction of the linkers to afatinib and ibrutinib, the resulting probes exhibited similar bioactivities to those of the parent compounds, and were shown to be suitable for simultaneous proteome profiling and live-cell imaging. Moreover, competitive labeling and competitive imaging can be general methods for *in situ* drug screening. We expect that these linkers, especially the azide- and TCO-containing linkers (**L8**/**10**), could be widely used in various irreversible inhibitors for drug screening and target identification.

We thank the National Natural Science Foundation of China (21602079, 21877050), the Science and Technology Program of Guangdong Province (2017A050506028), the Science and Technology Program of Guangzhou (201704030060, 201805010007) and the China Postdoctoral Science Foundation (2016M602611) for their financial support. We also thank Prof. Shao Q. Yao (NUS, Singapore) for the invaluable suggestions on this work.

Conflicts of interest

There are no conflicts to declare.

References

1 (*a*) J. G. Moffat, J. Rudolph and D. Bailey, *Nat. Rev. Drug Discovery*, 2014, **13**, 588–602; (*b*) M. Schenone, V. Dančík, B. K. Wagner and P. A. Clemons, *Nat. Chem. Biol.*, 2013, **9**, 232–240.

2 (*a*) D. S. Tyler, J. Vappiani, T. Cañeque, E. Y. N. Lam, A. Ward, O. Gilan, Y. C. Chan, A. Hienzsch, A. Rutkowska and T. Werner, *et al.*, *Science*, 2017, **356**, 1397–1401; (*b*) M. A. Miller and R. Weissleder, *Nat. Rev. Cancer*, 2017, **17**, 399–414; (*c*) P.-Y. Yang, K. Liu, M. H. Ngai, M. J. Lear, M. Wenk and S. Q. Yao, *J. Am. Chem. Soc.*, 2010, **132**, 656–666; (*d*) H. Shi, C. Zhang, G. Y. J. Chen and S. Q. Yao, *J. Am. Chem. Soc.*, 2012, **134**, 3001–3014.

3 (*a*) D. Medina-Cleghorn and D. K. Nomura, *Chem. Biol.*, 2014, **21**, 1171–1184; (*b*) C. G. Parker, A. Galmozzi, Y. Wang, B. E. Correia, K. Sasaki, C. M. Joslyn, A. S. Kim, C. L. Cavallaro, R. M. Lawrence, S. R. Johnson, I. Narvaiza, E. Saez and B. F. Cravatt, *Cell*, 2017, **168**, 527–541; (*c*) K. Lee, H. S. Ban, R. Naik and Y. S. Hong, *Angew. Chem., Int. Ed.*, 2013, **52**, 10286–10289.

4 (*a*) H. Guo and Z. Li, *MedChemComm*, 2017, **8**, 1585–1591; (*b*) K. Cheng, J. S. Lee, P. Hao, S. Q. Yao, K. Ding and Z. Li, *Angew. Chem., Int. Ed.*, 2017, **56**, 15044–15048; (*c*) Z. Li, P. Hao, L. Li, C. Y. J. Tan, X. Cheng, G. Y. J. Chen, S. K. Sze, H.-M. Shen and S. Q. Yao, *Angew. Chem., Int. Ed.*, 2013, **52**, 8551–8556; (*d*) Z. Li, D. Wang, L. Li, S. Pan, Z. Na, C. Y. J. Tan and S. Q. Yao, *J. Am. Chem. Soc.*, 2014, **136**, 9990–9998; (*e*) Z. Li, L. Qian, L. Li, J. C. Bernhammer, H. V. Huynh, J. S. Lee and S. Q. Yao, *Angew. Chem., Int. Ed.*, 2016, **55**, 2002–2006.

5 (*a*) M. Soethoudt, S. C. Stolze, M. V. Westphal, L. van Stralen, A. Martella, E. J. van Rooden and W. Guba, *J. Am. Chem. Soc.*, 2018, **140**, 6067–6075; (*b*) H. Guo, J. Xu, P. Hao, K. Ding and Z. Li, *Chem. Commun.*, 2017, **53**, 9620–9623; (*c*) D. Zhu, H. Guo, Y. Chang, Y. Ni, L. Li, Z.-M. Zhang, P. Hao, Y. Xu, K. Ding and Z. Li, *Angew. Chem., Int. Ed.*, 2018, **57**, 9284–9289; (*d*) B. Zheng, H. Guo, J. Xu, N. Ma, Y. Ni, L. Li, P. Hao, K. Ding and Z. Li, *Chem. – Asian. J*, 2018, **13**, 2601–2605.

6 (*a*) L. A. Honigberg, A. M. Smith, M. Sirisawad, E. Verner, D. Loury, B. Chang, S. Li, Z. Pan, D. H. Thamm, R. A. Miller and J. J. Buggy, *Proc. Natl. Acad. Sci. U. S. A.*, 2010, **107**, 13075–13080; (*b*) J. B. Smaill, G. W. Rewcastle, J. A. Loo, K. D. Greis, O. H. Chan, E. L. Reyner, H. D. Showalter, P. W. Vincent, W. L. Elliott and W. A. Denny, *J. Med. Chem.*, 2000, **43**, 1380–1397.

7 (*a*) A. T. Bender, A. S. Gardberg, A. Pereira, T. Johnson, Y. Wu, R. Grenningloh, J. Head, F. Morandi, P. Haselmayer and L. Liu-Bujalski, *Mol. Pharmacol.*, 2017, **91**, 208–219; (*b*) F. Solca, G. Dahl, A. Zoephel, G. Bader, M. Klein, C. O. Kraemer, F. Himmelsbach and E. G. R. Adolf, *J. Pharmacol. Exp. Ther.*, 2012, **343**, 342–350.

8 Y. Pang, K. Wang, Y. Wang, Z. Chenlin, W. Lei and Y. Zhang, *Chem.-Biol. Interact.*, 2018, **292**, 110–120.

9 S. Chang, L. Zhang, S. Xu, J. Luo, X. Lu, Z. Zhang, T. Xu, Y. Liu, Z. Tu, Y. Xu, X. Ren, M. Geng, J. Ding, D. Pei and K. Ding, *J. Med. Chem.*, 2012, **55**, 2711–2723.